Multi-Finger Haptic Rendering of Deformable Objects

Anderson Maciel, Sofiane Sarni, Olivier Buchwalder, Ronan Boulic, Daniel Thalmann

Virtual Reality Lab, Swiss Federal Institute of Technology, Switzerland

Abstract
The present paper describes the integration of a multi-finger haptic device with deformable objects in an interactive environment. Repulsive forces are synthesized and rendered independently for each finger of a user wearing a Cybergrasp force-feedback glove. Deformation and contact models are based on mass-spring systems, and the issue of the user independence is dealt with through a geometric calibration phase. Motivated by the knowledge that human hand plays a very important role in the somatosensory system, we focused on the potential of the Cybergrasp device to improve perception in Virtual Reality worlds. We especially explored whether it is possible to distinguish objects with different elasticities. Results of performance and perception tests are encouraging despite current technical and computational limitations.

Categories and Subject Descriptors (according to ACM CCS): I.3.5 [Computer Graphics]: Computational Geometry and Object Modeling: Physically Based Modeling, I.3.6 [Computer Graphics]: Methodology and Techniques: Interaction Techniques

1. Introduction

The human hand is extremely sophisticated in terms of motricity and perception; our success as a species is partly due to the vast range of abilities of the human hand. It is therefore logical that one wishes to transpose these abilities in Virtual Environments to exploit them for the manipulation of virtual prototypes. However, synthesizing a rich force information is not as simple as synthesizing an image. Specific stability problems arise whenever a haptic device is integrated to any 3D interaction task in Virtual Environment. So, the haptic interaction channel has long been reduced to the synthesis of a "point to model" interaction with devices such as the *Phantom* [MS94, Sen]. More recently, the *Cybergrasp*, a glove device with individual pulling ability for each finger has been proposed by the industry [Imm]. Despite its single directional force generation in the pulling direction and a smaller range of force, we hypothesize that the multiple finger perception can compensate for these limitations by allowing a relative perception from and action on the virtual object.

In the present article we describe an experimental setting establishing users' ability to discriminate virtual objects with various elasticities. A deformable tissue model serves to simulate a wide range of material that the user has to recognize by interacting with it. Two calibration stages are necessary: adjusting the size of the virtual hand and characterizing the deformable tissue model to behave like a given material in real-time. We first describe the deformable tissue model, then the experiment setting and the measurement results.

2. Related works

2.1. Haptic devices

New interaction devices appear and existent ones are improved unceasingly. We classify as interaction devices any device allowing interactive input and output in a computer system. We may also divide the many interaction devices in different subclasses from which we underline these three: graphical restitution, 3D capture, and force-feedback devices. For graphical restitution the 2D video monitor is still the most widely used, though for certain applications a cave or a head mounted display are necessary to improve immersion. For 2D capture the classical 2D mouse is the *de facto* standard. Several devices however extend mouse capabilities to 3D. An example is the *SpaceBall* [3DC] device, which allows data input for all space directions in a joystick-like mode and are mostly used in design applications or in research. Other systems are glove-like. A widely used device in Virtual Reality applications is the *Cyberglove* [Imm]. It allows capturing finger positions and angles accurately by means of optical fibers.

In the domain of force-feedback devices, there are also numerous recent improvements. However, there remains a great margin of evolution to make these products even more powerful [Bur03]. The first models to appear were associated to peripheral allowing input of 3D data. A very known example are the products type *Phantom* [MS94, Sen], composed of an articulated arm which permits to track a tool moving with 6 degrees of freedom in the space. Besides that tracking capacity, this device can resist to user's motion according to its position and orientation. The

main application of this device is the 3D design. In addition to *Phantom* devices, a certain number of exoskeleton-devices have also been commercialized. Such devices are placed on the body of the user, usually on its limbs, on which it applies forces. Due to their price and the lack of compatible applications, these devices are still used almost exclusively by advanced research centers. The *Cybergrasp* glove, developed by *Immersion* [Imm], is a product of exoskeleton type, composed of a metallic structure connecting every finger by a wire. It allows applying an independent force on each finger by tensioning the corresponding wire. This tool presents some limitations, like the direction of the force restricted to be always in the hand opening direction, the uncomfortable presence and the weight of the metallic part, the short cables connecting the glove to its driver, and the necessity to use it in combination with a 3D capture glove to be effective. Despite all these inconveniences, exploiting the hand makes this device very powerful due to the wide spectrum of human manual skills. This happens because the hand takes a larger part than any other in the somatosensory cortex [Dub02]. Neurons in this region are associated with somatic receptors in the skin. The classical representation of this mapping is the *homunculus* (Figure 1), where body parts sizes correspond to the proportion of somatosensory cortex dedicated to it. This shows how hand is important for sensation and perception and why a force-feedback glove is an interesting object of study for immersion issues in Virtual Reality.

Finally, we also mention an application area, the medical field, to which many specific devices have been designed. Such tools are used in surgery simulation and assisted surgery, and are a class of tools developing very quickly. In surgery simulation we can mention the *CathSim*, *LapSim*, *AccuTouch Endoscopy* and *AccuTouch Endovascular*, by *Immersion*. In assisted surgery, *DaVinci* and *Zeus* systems are already being used in hospitals but the feature of force feedback is not integrated so far.

Figure 1*: The Homunculus (adapted from Dubin [Dub02]). Body parts sizes are proportional to the somatosensory cortex area dedicated to it.*

2.2. Related work in haptics applications

A number of applications of the devices mentioned in section 2.1 and of new prototype devices has been developed and tested. These experiments are published in haptics literature beside other papers presenting new devices design. In this section, we present an overview of the applications of commercial or prototype devices; we are not especially interested in the design of the devices itself, but in their use to render appropriate sense of touch.

A brief classification could separate haptics applications in different groups according to interaction modality (single point vs. multi-finger) and the type of objects they deal with (rigid vs. deformable).

In the domain of single point haptics on rigid objects, Tarrin et al. [TCH*03] presented a stringed haptics device where a set of motors and pulleys tensions strings in order to control the position of an intersection point in the visual volume of a workbench for semi-immersive interactive tasks. Such point is attached to a user's finger and goes under collision detection with a virtual scene composed by rigid objects. Haptics forces are applied to avoid penetration. The device covers an important drawback of the Phantom device, generally used in that kind of applications, that is the visual perturbation caused by the Phantom's arm on the stereoscopic display.

Single point force-feedback devices have also been applied to render haptics from deformable objects. Mendoza and Laugier [ML01] presented a local topology model to obtain stable force-feedback using a 3 degrees of freedom Phantom device. Their goal was to use a virtual probe to interact on a highly deformable object model. They get high frequency haptics (1 KHz) even when physical simulation frequency is very low (10 Hz). Gregory *et al.* [GEL00] presented a 3D interface for interactively editing and painting a polygonal mesh using the Phantom device. The haptic feedback aids a user in free-form shape deformation allowing directly editing the surface.

Multi-finger applications are still not well documented. The literature is full of papers addressing the design and implementation of multi-finger haptic interfaces and devices, but their focus is not on their application on the sense of touch perception. The DigiHaptic presented by Casiez *et al.* [CPCS03] is a ground-based three degrees of freedom haptic device. It does not aim at imitating the hand anatomy and gesture but at gaining time in interaction with rigid 3D scenes. Springer and Ferrier [SF99], in turn, present a multi-finger hand-like haptic interface. They aim at rendering touch sensation to allow better controlling slave robotic or virtual fingers in grasping tasks. Another haptic interface, presented by Kawasaki *et al.* [KTT*03], is called Gifu and is still being perfectionated. It is similar to the human upper limb in shape and in motion ability. The arm is placed opposed to the human hand and is equipped with actuators in a way that it can be used as master or slave in virtual or real worlds.

3. The deformation model

Our approach to model soft tissues is presented in this section. It is based on a work of Jansson et al. [JV02] that has been used in computer-aided design. Their work exploits a generalized mass-spring model – which they call molecular model – where mass points are, in fact, spherical mass regions called molecules. Elastic forces are then established between molecules by a spring-like connection.

3.1. The force model

The model is described by two sets of elements: E, a set of spherical elements (molecules), and C, a set of connections between the elements in E (Eq. 1).

$$E = \{e_1, e_2, \cdots e_n\}, \; C = \{C_{e_1}, C_{e_2}, \cdots C_{e_n}\},$$
$$C_e = \{C_1, C_2, \cdots C_n\} \tag{1}$$

The model's behavior is determined by the forces produced on each element of E by each connection of C and some external forces.

$$\vec{F}_e = \vec{F}_G + \vec{F}_L + \vec{F}_C + \vec{F}_{collisions} \tag{2}$$

$$\vec{F}_G = m_e \vec{g} \tag{3}$$

$$\vec{F}_L = -\Pi r_e^{\,2} \rho |\vec{V}_e|^2 \frac{\vec{V}_e}{|\vec{V}_e|} \tag{4}$$

$$\vec{F}_C = \vec{F}_b + \vec{F}_d + \vec{F}_f \tag{5}$$

F_G: gravity (m_e is the mass of e and g is the gravity acceleration);
F_L: ambient viscous friction (r is the radius, ρ is the medium density and V is the velocity);
F_C: connection forces, see Eq. 6.

$$\vec{F}_C = \vec{F}_b + \vec{F}_d + \vec{F}_f \tag{6}$$

$$\vec{F}_b = \sum_{i=0}^{|C_e|} -k_c \left(|\vec{P}_e - \vec{P}_p| - l_c \right) \frac{\vec{P}_e - \vec{P}_p}{|\vec{P}_e - \vec{P}_p|} \tag{7}$$

$$\vec{F}_d = \sum_{i=0}^{C_e} -b_c \left(\vec{V}_\parallel \right) \tag{8}$$

$$\vec{V}_\parallel = \frac{\left(\vec{V}_e - \vec{V}_p \right) \cdot \left(\vec{P}_e - \vec{P}_p \right)}{|\vec{P}_e - \vec{P}_p|^2} \left(\vec{P}_e - \vec{P}_p \right) \tag{9}$$

$$\vec{F}_f = \sum_{i=0}^{C_e} -|\mu_e \vec{F}_N| \frac{\vec{V}_\perp}{|\vec{V}_\perp|} \tag{10}$$

$$\vec{F}_N = \vec{F}_b + \vec{F}_d \tag{11}$$

$$\vec{V}_\perp = \left(\vec{V}_e - \vec{V}_p \right) - \vec{V}_\parallel \tag{12}$$

F_b: elasticity (k_c is the spring Hooke's constant, l_c is the spring elongation, and P_e and P_p are the positions of the elements involved with connection c);
F_d: internal damping (b_c is the damping coefficient, P and V are respectively the positions and velocities of the elements involved with connection c);
F_f: sliding friction (μ_e is the friction constant for the element and F_N is the force normal to friction direction).

3.2. Mapping the material properties on a discretized volume

In a previous work [MBT03], we aimed at integrating properties of real materials, more specifically elasticity, to define the stiffness of the spring-like connections. The rheological standard to define the elasticity of a material is Young's modulus. Young's modulus is a property of a material, not of an object. So it is independent of the object's shape. However, when one discretizes an object by a set of springs, the stiffness k of every spring must be proportional to the fraction of the volume of the object it represents. It means that if a cube of side l_0 is compressed by a force F, it should shorten in the direction of the force, of the same elongation variation Δl both if it is represented by only one spring and if it is discretized by n springs (Figure 2). Equation 13 establishes the Young's modulus E from the knowledge of the elongation variation Δl, an applied force F, the length of the object in rest conditions l_0, and the cross-sectional area of the object A. Applying Equation 13 iteratively in the simulation loop we can minimize the difference between the obtained and the aimed E increasing or reducing the value of k's accordingly.

$$E = \frac{F \cdot l_0}{\Delta l \cdot A}, \tag{13}$$
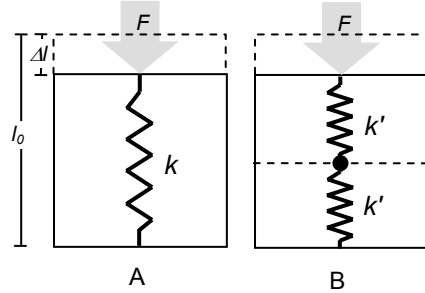
Figure 2: *2D approximation of an object discretization. Even for this simple two springs case, it is very difficult to find a direct relation between k and k'. An iterative solution is proposed using the equation 13 to obtain the same Young's modulus E of A for the discretized object B.*

4. Force-feedback model

Repulsion forces are calculated along the simulation every time the hand model collides with another object in the scene. The hand model status (position/orientation) is updated from data obtained from the *CyberGlove* capture device and all collisions on the hand model give rise to forces that are sent to the *CyberGrasp* force-feedback device.

4.1. Hand model

The hand is modeled as a classical hierarchical graph, where the joints are classical ball-and-socket with 3 degrees

of freedom. Initial arbitrary distances between joints are adjusted to user hand proportions by a calibration method.

4.2. Calibration

An automatic method is used to calibrate the virtual hand according to dimensions of the user's hand. This is done recording key positions of sensors (Figure 3) such that reference values 0 and 1 for minimal and maximal positions can be used to estimate angles and gain. Calculated values can be adjusted at any time by means of the user interface.

The final value for the angle of a sensor is calculated linearizing the raw value in the interval [0, 1], then multiplying the proportion index by the angle difference estimated between 0 and 1. A gain function allowing to correct the sensor linearity error can also be applied to the index.

$$Angle = f_{Gain}\left(\frac{rawVal}{ref_1 - ref_0}, gain\right) * angleDist \quad (14)$$

where $rawVal \in [\min, \max]$

$$f_{Gain}(ind, gain) = ind^{gain}, \text{ if } ind \in [0,1]$$
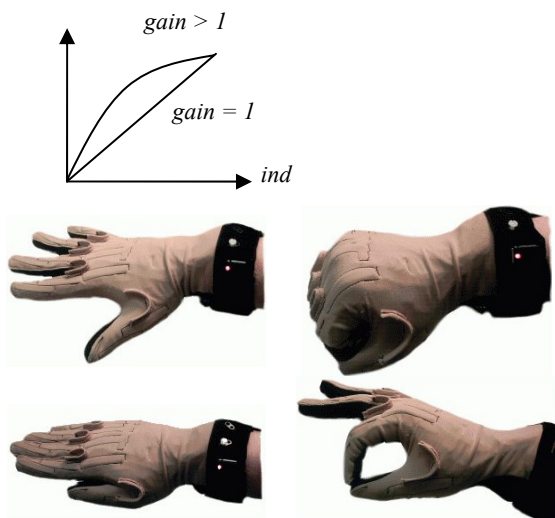$$f_{Gain}(ind, gain) = ind, \text{ if } (ind < 0, ind > 1)$$

Figure 3: *Key positions used for calibration.*

4.3. Collision detection and response

Efficient collision detection and response methods are required to simulate any physically realistic scene. In this work the interactions between two or more objects are handled by two separated methods, one for detecting collisions and the other for penetration avoidance.

A collision between spheres is one of the most straightforward situations to be detected. After optimizing the object-to-object test by a bounding box test, we simply

compare the distances between centers of candidate spheres with the sum of their radius. For collision avoidance we implement the classical Penalty Method [BW98]. A very small penetration is allowed and then a linear spring is created between the penetrating spheres to produce a repulsion force proportional to the penetration distance.

Objects subjected to collisions in our typical scene are a rigid ground, a deformable object and five fingertips represented by five spheres on which the feedback forces are measured and sent to the *Cybergrasp*.

4.4. Force smoothing

One of the new perspectives brought by the Cybergrasp device is that feedback forces can be synthesized independently for every finger. However, this same device imposes certain constraints which may limit its use. One of them is that the produced forces can be non-realistic in some situations. If the value of applied forces changes rapidly, the wires are tensioned and relaxed abruptly, which produces a non-natural sensation.

To minimize such effect a force smoothing method is needed. We developed a method to smooth force variation and integrated it into our software system. Our method is basically a low pass numerical filtering. Such method offers acceptable results making forces vary smoothly and naturally, but on the other hand it eventually causes a slight delay and must be hold by a thread of lower frequency in our implementation. In our case it is just a little above 100 Hz. We believe that it would be much more satisfactory to handle this problem on hardware.

4.5. Application

We developed an interactive application to test and evaluate our approach of using the two gloves and produce feedback forces from interaction with deformable objects. The basic application architecture is shown in Figure 4, and Figure 5 brings a screen shot. The user configures simulation parameters and gets visual feedback from the Graphical Interface. He sends actions to the system by means of the *Cyberglove* and receives force feedback by means of the *Cybergrasp*, both attached to the Capture/Force Peripherals module. The deformation model, in turn, is implemented in the Deformation Engine module. The Main System module coordinates and synchronizes the other modules.
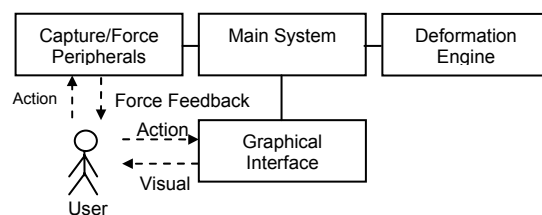

Figure 4: *High-level diagram of the application architecture.*

We made use of separation of processes all over the system implementation. Force feedback process runs asynchronously with the display, for example. It allowed us to reduce the display frequency at the same time that the force update frequency was kept high to avoid vibrations on the device.
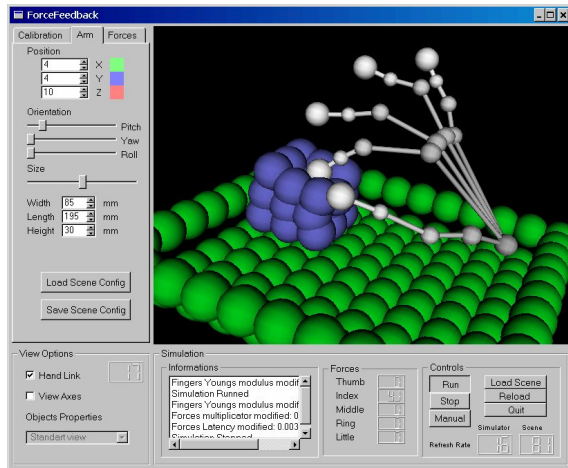

Figure 5: *Graphical interface of the application.*

5. Tests and Results

Two different tests have been conducted with the system. A performance test aimed at evaluating the implementation itself, the processes separation in threads and how we could improve the models and the implementation to gain in performance. A perception test aimed at evaluating the capacity of the *Cybergrasp* device to produce realistic sensations, and identifying its potential strengths and weaknesses for perception issues in Virtual Reality.

5.1. Performance test

We created four scenes of different complexities (Figure 6) and simulated them on a dual Xeon 1700 MHz with 1 GB of RAM. The results in terms of refresh rates for each thread are visible in Table 1.

The different values on the table show that the *display* thread and the *main* thread update frequencies are dependent of the scene complexity. In which concerns the *display* it can be easily explained. However, for the *main* thread this fact seems surprising. In fact, even if the display is independent and can be executed in parallel, these two threads have to be synchronized regularly. For complex scenes, the main thread must wait more often for the display, it is then slowed down. In spite of this, the multi-threading approach is not called into question because without it the display would fall down to rates equal or below the main thread, which would make the simulation non-interactive.

The frequency of the *forces update* thread is practically stable in all scenes. It is less dependent on the other

threads. We notice, however, that its frequency has a tendency to diminish when the scene is more complex. It is due to the increased number of swaps between the different threads.

In practice, the main thread cannot go much under 20 Hz so that the application runs in an acceptable way and the user sensation is sufficiently realistic. About the visual display, it does not penalize the global system performance. Because the objects are very simple, the display time can be neglected when compared to the other tasks.
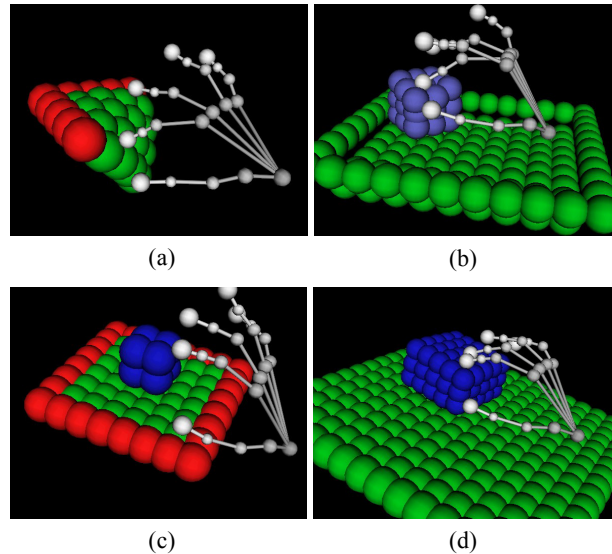

(a)   (b)

(c)   (d)

Figure 6: *Four scenes of different complexities. (a) has 25 molecules (9 are fixed and 16 deformable), (b) has 148 molecules (121 are fixed and 27 deformable), (c) has 72 molecules (28 are fixed and 42 deformable) and (d) has 300 molecules (225 are fixed and 75 deformable).*

	Scene a	Scene b	Scene c	Scene d
Main thread	35	19	15	7
Display thread	131	90	79	38
Forces update	403	424	430	440

Table 1: Refresh rates for main, display and forces threads (in Hz)

5.2. Perception test

In order to evaluate haptic rendering by the application, we made up an experiment where users were challenged to recognize objects of different elasticities. This test was conducted with 8 persons. We used 4 real samples of deformable materials with different deformation behavior, though not too much different. The samples were cubes of 5 cm long edges made of 2 different types of sponge and 2 others of foam. These real objects were related to 4 virtual cubes discretized in 9 molecules (3x3x3). These latter were calibrated modifying their Young's modulus in order to correspond to every real cube. We also made the

assumption that friction constant could be neglected and used the same friction parameter for all virtual cubes.

We asked the testers to firstly manipulate the real objects in a very controlled way: pressing one or more fingers on their upper surface keeping the wrist fixed on a table. Then we asked them to put them in order from the softest to the hardest. After that, they tested in the same way the virtual objects and were asked to establish the sensation correspondences between the real and the virtual cubes. Figure 7 illustrates the test.
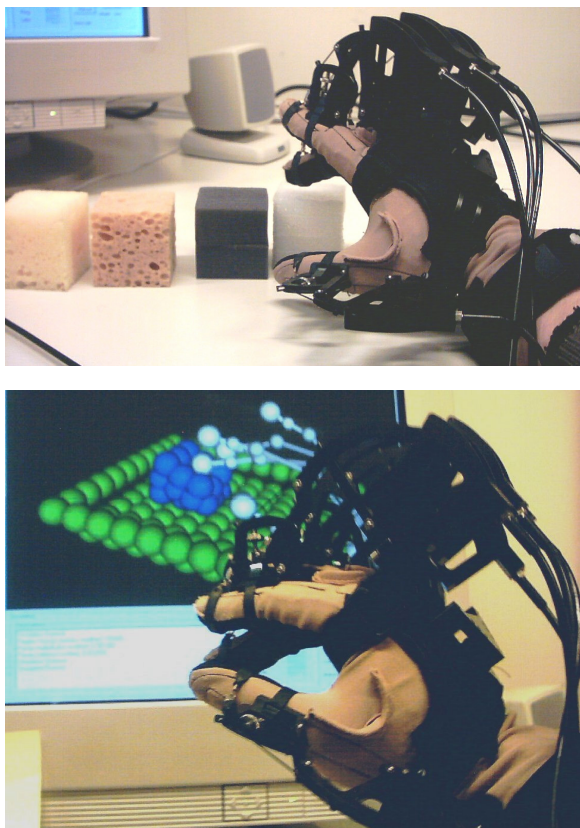

Figure 7: *Testing reaction force of different objects*

Number of good correspondences	0	2	4
Percentage (%)	12.5	12.5	75

Table 2: *Perception tests results*

Most of the users (75%) have correctly recognized the 4 virtually rendered objects by matching them with corresponding real objects. In other cases, errors come from inversion of two objects that are close in elasticity. 12.5% have made 1 inversion and 12.5% have made 2 inversions.

We have also noticed that visual feedback affects users' sensations. This effect, called pseudo-haptic feedback [LCK*00] is known. The percentage of wrong correspondences increases when the users are asked to make the test without looking at the screen. We believe that besides the pseudo-haptic feedback, the fact that the objects

move and a "blind user" looses contact with them, has an important influence to the increased number of wrong correspondences. A new test setup should be prepared to evaluate these effects.

6. Conclusion

In this work we presented the integration of a multi-finger haptic device, the *Cybergrasp*, with deformable objects in an interactive environment. We investigated the potential of this tool to improve perception in Virtual Reality worlds. Motivated by the knowledge that human hand plays a very important role in the somatosensory system, we invited users to identify from a set of virtual deformable objects their correspondents in a set of real objects.

The success of most of the tests allows us to conclude positively on the use of the device for many applications in Virtual Reality. However, we also identified a set of drawbacks that require improvements to be done on the device. We may mention the lack of force smoothing procedures implemented in hardware, and the direction of applied forces that is limited to the hand opening direction. In addition, other factors, like tactile and visual feedback, seem to play an important role besides the force-feedback.

Some of the potential applications for this tool, involving both deformable and rigid objects, are penetration avoidance in virtual worlds, virtual sculpture on different materials (plastic deformation), or palpation on virtual bodies in orthopedic Medicine. Nevertheless, many applications are not possible, especially all which require very high frequencies like vibrations or contact with very irregular and very hard deformable objects. For those, the devices type *Phantom* are more indicated.

7. Acknowledgements

References

[3DC]   3Dconnexion.
          http://www.3dconnexion.com/products.

[Bur03]   BURDEA G. C.: Haptic feedback for virtual reality. In *In Virtual Reality and PrototypingWorkshop* (Laval (France), June 2003).

[BW98]   BARRAF D., WITKIN A.: Physically based modelling. In *SIGGRAPH'98 Course Notes* (1998).

[CPCS03] CASIEZ G., PLÉNACOSTE P., CHAILLOU C., SEMAIL B.: The DigiHaptic, a new three degrees of freedom multi-finger haptic device. In *Virtual Reality International Conference* (May 2003), pp. 35–39.

[Dub02] DUBIN M.: *How the brain works*, first edition. Blackwell Science, 2002.

[GEL00] GREGORY A., EHMANN S., LIN M. C.: in-Touch: interactive multiresolution modeling and 3d painting with haptic interface. In *Proceedings of IEEE International Conference on Virtual Reality 2000* (2000).

[Imm] Immersion. http://www.immersion.com.

[JV02] JANSSON J., VERGEEST J.: A discrete mechanics model for deformable bodies. *Journal of Computer-Aided Design 34*, 12 (2002), 913–928.

[KTT*03] KAWASAKI H., TAKAI J., TANAKA Y., MRAD C., MOURI T.: Control of multi-fingered haptic interface opposite to human hand. In *Proceedings of the International Conference on Intelligent Robots and Systems* (Las Vegas, 2003).

[LCK*00] LECUYER A., COQUILLART S., KHEDDAR A., RICHARD P., COIFFET P.: Pseudo-haptic feedback: can isometric input devices simulate force feedback? In *Proceedings of IEEE Virtual Reality 2000* (New Jersey, 2000), pp. 83–90.

[MBT03] MACIEL, A., BOULIC, R., THALMANN, D.: Deformable Tissue Parameterized by Properties of Real Biological Tissue. In *Proc. International Symposium on Surgery Simulation and Soft Tissue Modeling*, Juan-les-Pins, France, Springer-Verlag, 2003, pp.74-87.

[ML01] MENDOZA C., LAUGIER C.: Realistic haptic rendering for highly deformable virtual objects. In *Proceedings of IEEE International Conference on Virtual Reality 2001* (2001), pp. 264–269.

[MS94] MASSIE T. H., SALISBURY J. K.: The phantom haptic interface: A device for probing virtual objects. In *Proceedings of ASME Winter Annual Meeting Symposium. Haptic Interfaces for Virtual Environment and Teleoperator Systems* (1994).

[Sen] Sensable technologies. http://www.sensable.com.

[SF99] SPRINGER S., FERRIER N.: Design of a multi-finger haptic interface for teleoperational grasping. In *ASME Int'l Mech. Eng. Congress and Expo* (November 1999).

[TCH*03] TARRIN N., COQUILLART S., HASEGAWA S., BOUGUILA L., SATO M.: The stringed haptic workbench: a new haptic workbench solution. In *Proceedings of Eurographics* (2003).